CFD-Based Lagrangian Multiphase Analysis of Particulate Matter Transport in an Operating Room Environment

Ahmet ÇOŞGUN * and Onur GÜNDÜZTEPE

Posted Date: 29 July 2025

doi: 10.20944/preprints202507.2346.v1

Keywords: CFD; lagrangian multiphase method; particulate matter transport; operating room air quality; HVAC system optimization; ISO Class 7

 doi:10.20944/preprints202507.2346.v1

Article

CFD-Based Lagrangian Multiphase Analysis of Particulate Matter Transport in an Operating Room Environment

Ahmet Çoşgun [1,*] and Onur Gündüztepe [2]

[1] Akdeniz University, Faculty of Engineering, Department of Mechanical Engineering, Antalya, Turkey
[2] Akdeniz University, Institute of Natural and Applied Science, Department of Mechanical Engineering, Antalya, Turkey
* Correspondence: acoskun@akdeniz.edu.tr

Abstract

Maintaining air quality in operating rooms is critical for infection control and patient safety. Particulate matter, originating from surgical instruments, personnel, and external sources, is influenced by airflow patterns and ventilation efficiency. This study employs Computational Fluid Dynamics (CFD) simulations using Simcenter STAR-CCM+ 2410 to analyze airflow and particulate behavior in a surgical-grade operating room. A steady-state solver with the k-ε turbulence model was used to replicate airflow, while the Lagrangian multiphase method simulated particle trajectories (0.5 μm, 1 μm, and 5 μm). The simulation results demonstrated close agreement with the experimental data, with average errors of 17.3%, 17.7%, and 39.7% for 0.5 μm, 1 μm, and 5 μm particles, respectively. These error margins are considered acceptable given the device's 10% measurement sensitivity and the observed experimental asymmetry—attributable to equipment placement—which resulted in variations of 17.2%, 18.0%, and 26.5% at corresponding symmetric points. Collectively, these findings support the validity of the simulation model in accurately predicting particulate transport and deposition within the operating room environment. Findings confirm that optimizing airflow can achieve ISO Class 7 cleanroom standards and highlight the potential for future studies incorporating dynamic elements, such as personnel movement and equipment placement, to further improve contamination control in critical environments.

Keywords: CFD; lagrangian multiphase method; particulate matter transport; operating room air quality; HVAC system optimization; ISO Class 7

1. Introduction

The management of air quality in operating rooms is critical for maintaining sterile conditions and minimizing the risk of postoperative infections. Achieving compliance with air cleanliness standards, such as ISO Class 7, requires a comprehensive understanding of airflow dynamics and particulate transport mechanisms. Contaminants in operating rooms primarily originate from sources such as medical personnel movement, surgical equipment, and patients. Studies have shown that human skin, clothing, and activities—such as periodic bending or movements of surgeons—significantly influence the distribution of bacteria-carrying particles within the surgical field, potentially leading to contamination (Friberg et al., 2001; Brohus et al., 2006; Chow and Wang, 2012; Annaqeeb et al., 2021).

In enclosed environments, the primary source of airborne bacteria is human presence, with skin particles, respiratory emissions, and clothing contributing to aerosolized particulates (Mackintosh et al., 1978; Hospodsky et al., 2012). The behavior and dispersion of these particles largely depend on their size and the airflow patterns within the room. For instance, larger particles tend to settle quickly due to gravitational effects, whereas smaller particles remain suspended and can be transported over

 doi:10.20944/preprints202507.2346.v1

longer distances (Li and Hou, 2003; Nazaroff, 2004). Additionally, while surgical activity and surgeon movement often leads to higher levels of airborne microbial contamination, proper ventilation systems can effectively maintain acceptable air quality (Pasquarella et al., 2007; Saidi et al., 2011; Balocco et al., 2014; Pasquarella et al., 2020). The configuration and positioning of medical equipment can also significantly influence contaminant dispersion in operating rooms, particularly under unidirectional downflow conditions (Aganovic et al., 2019).

Computational Fluid Dynamics (CFD) has emerged as a powerful tool for simulating and analyzing complex airflow and particle dynamics in controlled environments. CFD methods, particularly the Eulerian approach, are widely used to model air and particle flow, providing detailed insights into distribution patterns and deposition rates (Chow and Wang, 2012; Balocco et al., 2014; Çoşgun and Koyun, 2025). Previous studies have demonstrated the successful application of CFD in evaluating the effectiveness of ventilation systems in minimizing particle dispersion and reducing contamination risks in operating rooms (Chow and Wang, 2012). Moreover, numerical simulations employing the k-ε turbulence model have been utilized to analyze the impact of airflow systems on air quality and contaminant control in surgical environments (Balocco et al., 2014; Çoşgun and Koyun, 2025). On the other hand, advanced turbulence models such as Direct Numerical Simulation (DNS) and Large Eddy Simulation (LES) provide higher accuracy but are often associated with extremely high computational costs (Chow and Wang, 2012).

This study applies steady-state CFD simulations using the k-ε turbulence model to evaluate airflow and particulate matter behavior in an operating room. The primary objective is to assess how airborne particles of varying sizes (0.5 μm, 1 μm, and 5 μm) behave under standard surgical conditions, with a focus on identifying regions of accumulation that may contribute to infection risk. It is hypothesized that airflow patterns within the room, influenced by ventilation design and equipment layout, significantly affect particle distribution. This study assumes a one-way coupling approach, where particles are influenced by the continuous air phase but do not affect the airflow. Additionally, particle-particle interactions are considered negligible, meaning no collisions or agglomeration effects are accounted for. The Lagrangian multiphase method was employed to simulate particles with diameters of 0.5 μm, 1 μm, and 5 μm, investigating their accumulation and distribution under standard surgical conditions. The simulation results were validated against experimental data, providing valuable insights for optimizing air quality management in operating rooms. Furthermore, this work contributes to the development of infection control strategies by addressing the need for advanced simulations that incorporate dynamic factors such as personnel movement and variable contaminant sources.

2. Materials and Methods

This study was conducted in an operating room at a private hospital in Antalya, with a total surface area of 49.7 m^2 and a ceiling height of 3 m, resulting in a volume of approximately 149 m^3. The general view of the operating room is shown in Figure 1 below.

Figure 1. Operating room view of a private hospital

 doi:10.20944/preprints202507.2346.v1

The operating room's airflow system includes a High Efficiency Particulate Air (HEPA) filtered laminar flow unit positioned above the surgical area to provide clean air intake. The operating room walls also contain air outlet vents that exhaust air from the room.

The view of the operating room defined in the simulation is shown in Figure 2. The operating room has an air inlet vent measuring 2400 × 1800 mm for the laminar flow unit on the ceiling. There are a total of four air outlet vents, each measuring 310 × 310 mm, on two opposite walls of the operating room.

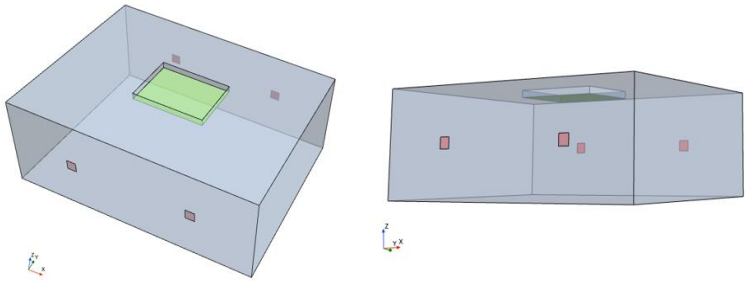

Figure 2. 3D view of the operating room simulation area from different angles

a) Particle Count Measurements:

In the study, particulate matter measurements were conducted using the Solair 3100E device. Below, Figure 3 shows the appearance of the Solair measurement device.

Figure 3. Solair 3100E particulate matter measurement device appearance

The Solair 3100E device utilizes the Optical Particle Counter (OPC) method for particle counting. It operates with Extreme Life Laser Diode Technology to optically detect airborne particles. Capable of counting particles ranging from 0.3 µm to 10 µm, the device complies with cleanroom standards and holds ISO 21501-4 certification, allowing simultaneous display of different particle sizes. The technical specifications of the Solair 3100E device are provided in Table 1.

Table 1. Technical specifications of the solair 3100e particulate matter measurement device

Specification	Details
Measurement Range	0.3 - 10 µm
Measurement Principle	Laser light scattering technique
Accuracy	±10% for particle concentration measurements
Detection Limit	Minimum detectable particle size: 0.3 µm
Applications	Industrial, laboratory, hospital, cleanroom, HVAC

b) Simulation Approach

Computational Fluid Dynamics (CFD) simulations were conducted using Simcenter STAR-CCM+ 2410 software to analyze airflow and particulate matter behavior in the operating room. A steady-state solver was used for velocity profile modeling, and the k-ε turbulence model was applied to accurately represent turbulent airflow. This model was chosen for its robustness, computational efficiency, and proven reliability in predicting general turbulent flow behavior in enclosed

 doi:10.20944/preprints202507.2346.v1

environments such as rooms and ventilation systems. Once the airflow reached a steady state, the solver was frozen, and the Lagrangian multiphase solver was activated to simulate particle trajectories. This decoupling of the fluid velocity solver from the particle transport solver is appropriate for cases with low particle volume fractions, where the influence of particles on the continuous phase is minimal. A one-way coupling approach was therefore employed, in which particles are affected by the airflow but do not alter it. Particle-particle interactions were also neglected, assuming a dilute particle dispersion without significant collisions or agglomeration.

The computational domain was meshed using a polyhedral mesher, which is well-suited for capturing complex velocity fields due to its multidirectional cell faces that enhance numerical stability and accuracy. The mesh was refined at critical regions to resolve flow gradients effectively. Specifically, a cell size of 2.5 cm was applied at the inlet and outlet, while the wall regions used a slightly coarser cell size of 5 cm. Away from surfaces, the cell size was gradually increased up to 20 cm to reduce computational cost without compromising solution accuracy near areas of interest. To better capture the boundary layer near wall surfaces, two prism layers were added with a total thickness of 2 cm and a stretching ratio of 1.5, ensuring accurate resolution of near-wall flow behavior. The final mesh consisted of approximately 1.5 million cells, balancing computational efficiency with adequate resolution for accurate flow prediction.

The air was assumed to have a constant density of 1.18415 kg/m^3 and a constant viscosity of 1.85508×10^{-5} Pa·s at a temperature of 298.15 K and a pressure of 101,325 Pa. Although temperature variations can induce natural convection and influence particle dynamics, this study assumes a constant temperature within the room. The simulations were conducted in an empty operating room, where thermal effects were considered negligible. Therefore, the segregated fluid isothermal model was used as the energy model. Experimentally measured particle densities in air from various locations around the world are obtained from previous studies and given in Figure 4. In this simulation study, particle density assumed as 1.66 g/cm3, slightly lower than maximum (1.64 g/cm3) particle density in Figure 4. In this study, particle-particle interactions were assumed to be negligible, enabling independent analysis of different particle sizes. Three particle size groups—0.5 μm, 1 μm, and 5 μm—were selected based on ISO Class 7 classification criteria. Each group was simulated separately using a Lagrangian multiphase solver. Gravitational acceleration was defined as -9.81 m/s^2 in the z-direction.

Figure 4. Global distribution of particle density in air. Values are taken from various sources: Texas (Hand and Kreidenweis 2002), Pittsburgh (Khlystov et al. 2004), Augsburg (Pitz et al. 2008), Beijing (Hu et al. 2012), Massachusetts (Kassianov et al. 2014) and Shouxian (Li et al. 2018)

In the study, the simulation was initially performed until steady state was reached, with an air inlet boundary condition of 0.24 m/s velocity from the laminar flow unit and a 0 Pa air pressure boundary condition at the four vents on the walls. This allowed for the determination of the velocity and pressure distribution of the air in the operating room at steady state. Assuming that the velocity distribution of the air was unaffected by the particles, the velocity and pressure distributions obtained from the steady-state solution on the air side were fixed, and the solver on the air side was frozen.

 doi:10.20944/preprints202507.2346.v1

Only the simulation of Lagrangian particles was then performed. The simulations of the Lagrangian particles were carried out separately according to their sizes.

In the simulation, particulate matter was initiated from the surface of the laminar flow unit's air inlet with a certain number of airflows moving in the same direction and at the same speed. The trajectory of the particles was calculated considering the effects of gravity and airflow. To accurately model the drag forces exerted by the air flow on the particles, a drag force model was used, and the drag coefficient was determined using the Schiller-Naumann correlation (Schiller and Naumann 1933). Additionally, to ensure precise representation of particle motion, a shear lift force model was applied, and the shear lift force coefficient was calculated using the Sommerfeld method (Sommerfeld 2000). A turbulent dispersion model, based on principles outlined in Gosman and Ioannides (1983), was implemented to simulate the effects of turbulent flow on particle distribution. Particle trajectories were obtained as the simulation result.

The multidimensional approach in the simulation ensures that the dynamics of particulate matter are comprehensively simulated under the combined effects of gravity, aerodynamics, and turbulent flow. Instead of using a time-dependent approach with continuous particle feeding, the particles were fed into previously obtained steady state air flow solution domain, and their trajectories were simulated. This reduced the number of particles to be simulated, significantly decreasing the required time and computational resources for the simulation. However, additional processing was needed to obtain volumetric particle count values from the simulation results. By using the particle path data obtained from the simulation, the number of particles passing through any surface in the simulation can be determined. The particle count obtained from surfaces placed in the simulation can be converted into volumetric particle count values, similar to the experimental measurements, by using the ratio of the number of particles fed per unit area from the laminar flow unit to the experimentally measured particle count just below the laminar flow unit. This method allows for a direct comparison of simulation results with experimental data.

c) ISO Particulate Standards

In evaluating the particulate concentrations in the operating room, the ISO 14644-1 standard, which defines cleanroom standards, has been used as a reference. Table 2 summarizes the ISO classification criteria for different particle sizes. These standards were used as a benchmark to determine the air cleanliness level obtained in the simulated operating room.

Table 2. ISO classification for particle matter concentrations

ISO Class	≥0.1 µm	≥0.2 µm	≥0.3 µm	≥0.5 µm	≥1 µm	≥5 µm
ISO 1	10	-	-	-	-	-
ISO 2	100	24	10	-	-	-
ISO 3	1,000	237	102	35	-	-
ISO 4	10,000	2,370	1,020	352	83	-
ISO 5	100,000	23,700	10,200	3,520	832	29
ISO 6	1,000,000	237,000	102,000	35,200	8,320	293
ISO 7	-	-	-	352,000	83,200	2,930
ISO 8	-	-	-	3,520,000	832,000	29,300
ISO 9	-	-	-	35,200,000	8,320,000	293,000

d) Validation and Analysis

Simulation results were compared with experimental velocity and pressure measurements obtained from the operating room. By evaluating particulate matter accumulation patterns, potential contamination areas were identified, and the accuracy of the simulation was examined based on its agreement with experimental data. This methodological framework serves as a foundation for future studies investigating more complex scenarios, such as optimizing operating room airflow and

 doi:10.20944/preprints202507.2346.v1

particle distribution by altering personnel and equipment positions in room and analyzing alternative air inlet-outlet configurations.

3. Results

As a result of the simulation study, air pressure, airflow velocity, and the trajectories of particulate matter within the operating room were obtained. Air pressure and airflow velocities were compared with experimental data. The trajectories of particulate matter obtained from the simulation were analyzed by determining the number of intersections with measurement surfaces, which were then converted into volumetric count data for comparison with experimental results. The results are presented under specific headings.

a) Air Pressure Distribution

The pressure distribution in the operating room is shown in Figure 5. The pressure values range between 7.12 and 7.19 Pa.

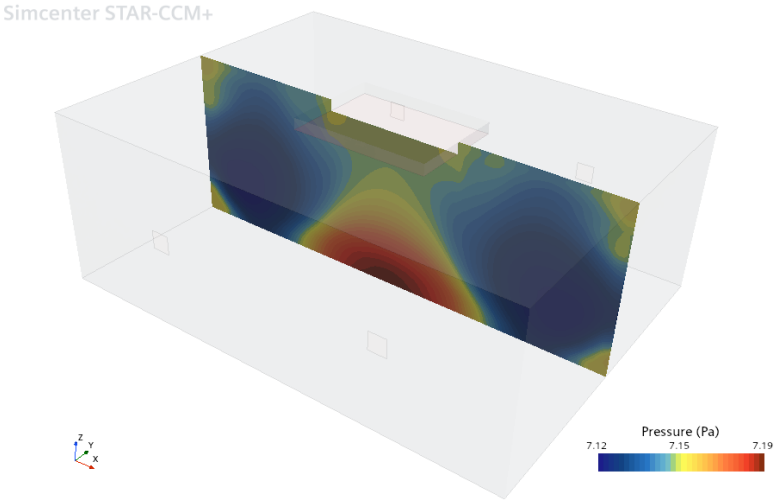

Figure 5. Pressure distribution along the plane section passing through the center of the operating room

The pressure distribution obtained from the simulation, ranging between 7.12 - 7.19 Pa, meets the minimum pressure difference criterion of $P > 6$ Pa, which is required to maintain positive pressure in the operating room. Additionally, the simulation results show a high correlation with the experimental data, which was measured as 7 Pa. This confirms that the numerical model accurately predicts the pressure conditions. Positive pressure plays a critical role in preventing contaminants from infiltrating the operating room, which is vital for maintaining a sterile environment.

b) Velocity Profiles

The experimental velocity results measured at various points 140–300 mm below the laminar flow unit are presented in Table 3. The recorded velocities range between 0.21 and 0.26 m/s, with an average velocity of 0.24 m/s.

Table 3. Experimental air velocity measurements.

Velocity (m/s)	**X (mm)**							
Y (mm)	**300**	**600**	**900**	**1200**	**1500**	**1800**	**2100**	**2400**
300	0.22	0.23	0.25	0.22	0.25	0.24	0.23	0.23
600	0.22	0.25	0.26	0.23	0.24	0.24	0.23	0.25
900	0.23	0.22	0.25	0.24	0.26	0.25	0.23	0.24

 doi:10.20944/preprints202507.2346.v1

1200	0.24	0.25	0.23	0.23	0.23	0.22	0.21	0.25
1500	0.23	0.23	0.22	0.24	0.24	0.25	0.22	0.26
1800	0.23	0.22	0.24	0.23	0.23	0.22	0.25	0.24

In the vertical section of the operating room shown in Figure 6, the velocity near the inlet of the laminar flow unit is approximately 0.24 m/s. These results are consistent with the experimental measurement data presented in Table 3. In the circulation areas between the laminar flow unit and the walls, the air velocity varies between 0 and 0.3 m/s. This velocity distribution indicates that laminar flow is effectively maintained in the area beneath the laminar flow unit.

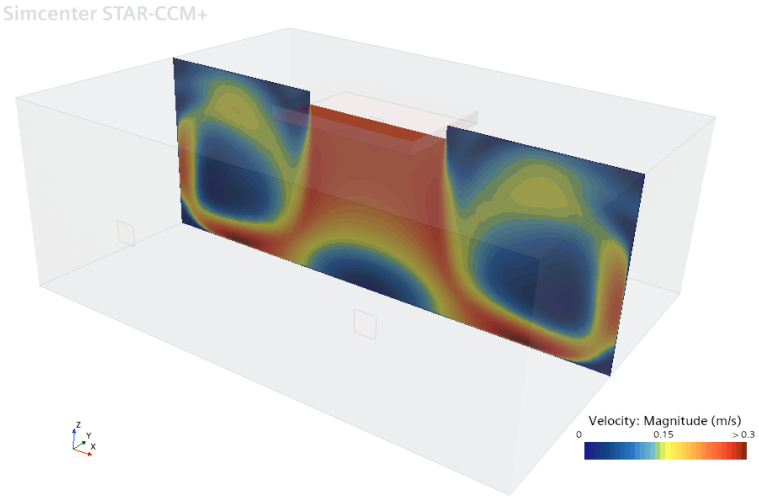

Figure 6. Air velocity magnitude distribution along the vertical plane section passing through the center of the operating room

In Figure 7, the velocity distribution in the horizontal section of the operating room at a height of 1.2 m above the floor shows that the air velocity is 0.24 m/s beneath the laminar flow unit and near the walls. However, in areas close to the outlet vents, the air velocity increases to approximately 0.3 m/s. Throughout the operating room, the velocity variation is within the range of 0–0.3 m/s, and the resulting velocity distribution reveals the circulation zones inside. The simulation results indicate that the airflow design effectively maintains a consistent air velocity in the critical operating area.

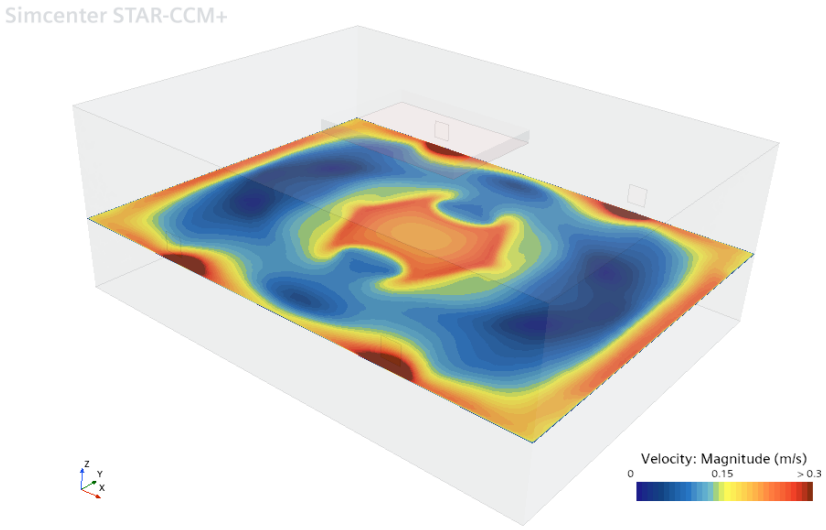

Figure 7. Air velocity magnitude distribution along the horizontal plane section passing through the center of the operating room.

 doi:10.20944/preprints202507.2346.v1

The air velocity results obtained through simulation analysis at the previously experimentally measured points are presented in Table 4.

Table 4. Simulation Air Velocity Results.

Velocity (m/s)	X (mm)							
Y (mm)	**300**	**600**	**900**	**1200**	**1500**	**1800**	**2100**	**2400**
300	0.241	0.242	0.241	0.240	0.240	0.242	0.243	0.241
600	0.244	0.241	0.240	0.240	0.240	0.240	0.241	0.244
900	0.242	0.241	0.240	0.240	0.240	0.240	0.241	0.242
1200	0.242	0.241	0.240	0.240	0.240	0.240	0.241	0.242
1500	0.244	0.241	0.240	0.240	0.240	0.240	0.241	0.244
1800	0.240	0.242	0.242	0.240	0.240	0.241	0.242	0.242

When Table 4 is examined, the simulation results show that the air velocity ranges between 0.240 – 0.244 m/s, while the experimental results range between 0.21 – 0.26 m/s (Table 3). The larger variation in the experimental results may be due to the shape of the exit plate at the laminar flow unit vent. Specifically, the grid holes on the air exit vent plate and the internal structure of the laminar unit can cause the exit air velocities to vary depending on the location. In the simulation, since the vent plate geometry was not considered in this study, a regular air velocity profile was observed near the inlet boundary, as expected.

c) Distribution and Accumulation of Particulate Matter

In the simulation, the trajectories of Lagrangian particulate matter were calculated over a period of 100 minutes. A particle density of 10,000 particles/m² was defined at the laminar flow vent, which corresponds to 43,201 particulate matter particles. Instead of continuous particle feeding, a one-time particle feed was implemented in the study. The paths followed by the particles, along with data such as the number of times they passed through specific surfaces, were used to determine the volumetric particle count.

In the simulation of the operating room, Figure 8 shows the paths followed by 0.5 μm diameter particles over 50 seconds after being released from the laminar flow unit. The paths of the particles within the air are color-coded based on time. In the dark blue areas, the particles indicate their entry position into the operating room. The blue particles that descend to the floor are directed toward the side walls. Around 25 seconds, the yellow particles are seen moving upward from the side wall edges. Similarly, the red dust particles reach the ceiling at around 45 seconds and head toward the laminar flow vent. By 50 seconds, the particles are seen moving downward from the laminar flow vent. Some particles are observed exiting the room through the air exit vents.

 doi:10.20944/preprints202507.2346.v1

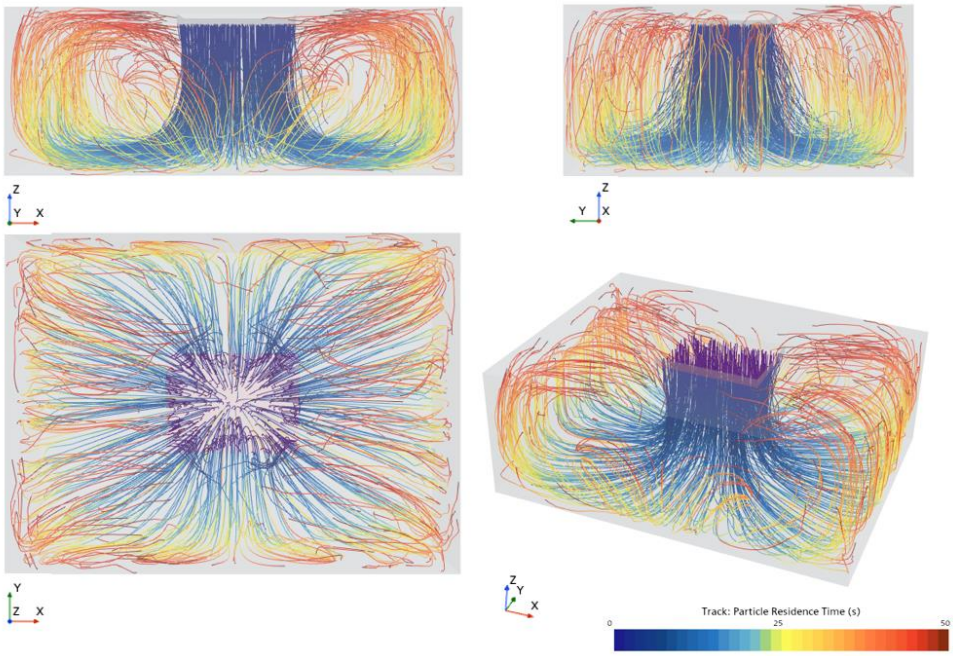

Figure 8. Particle trajectories of 0.5 μm diameter particles from 0 to 50 seconds.

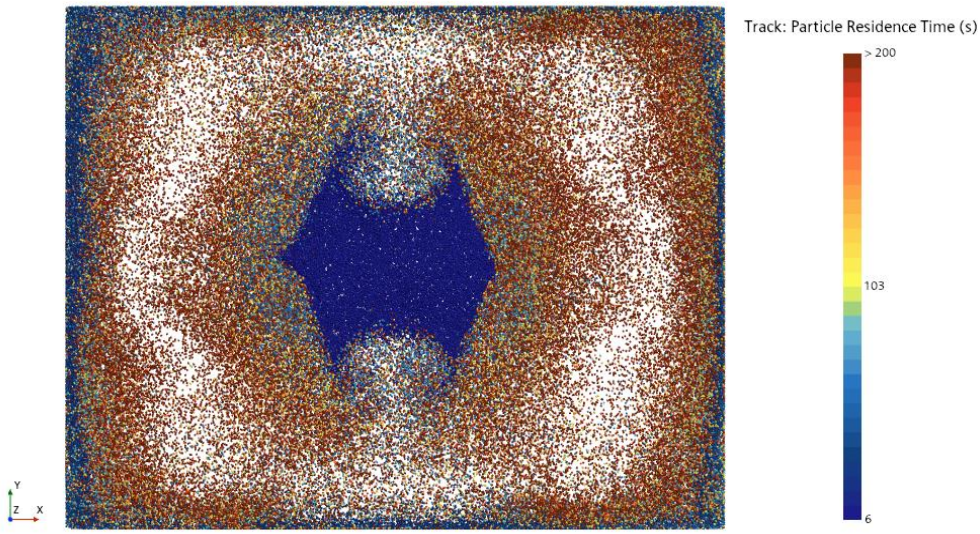

Figure 9. Particle trajectory intersection points of 0.5 μm diameter particles in the z = 1.2 m plane, color-coded by particle residence time.

The plane section is placed 1.2 m above the operating room floor, and the intersection points of particulate matter over 10 minutes crossing this plane section are visualized in Figure 9. According to Figure 8, the particles begin circulating within the operating room after crossing the plane 6 seconds later, especially moving between the walls and the laminar flow area. Some particles leave the operating room through suction vents located on the side wall, which is normal to the y-axis. As a result, the circulation of dust particles is lower in regions near these side walls compared to other walls, and the circulation of dust particles is especially less in the area between the two exit vents on the same wall. This situation highlights the differences in the movement and accumulation areas of particulate matter within the operating room.

In the experimental study, the locations where particulate matter measurements were made at a height of 1.2 m are shown in the regions of Figure 10. The height of 1.2 meters was selected because it approximately corresponds to the nose or eye level of an operator during surgical operation. This allows the simulation results to be compared with what a surgeon or medical staff member would

 doi:10.20944/preprints202507.2346.v1

realistically observe during an operation, ensuring relevance to actual working conditions in the operating room. The measurement duration at each location was set to 1 minute. The particle count measurements are expressed in particles/m³. These data were used to assess the particle density in the room and compare it with the simulation results.

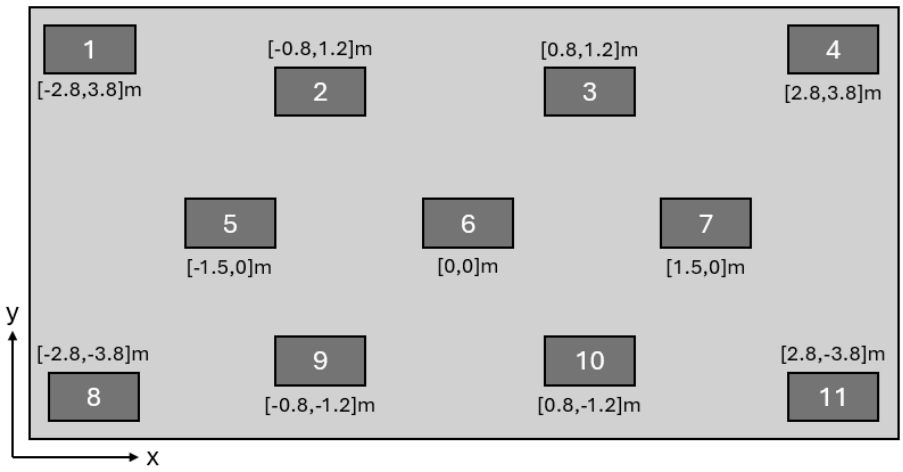

Figure 10. Particle count measurement locations with coordinates in the experimental study

In the simulation study, the number of particles passing through the surfaces positioned at a height of 1.2 m in the regions numbered in Figure 10 was recorded. The number of particles passing through each surface was divided by the surface area to obtain the number of particles passing per unit area. Using the ratio between the volumetric measurement value at the laminar flow unit inlet and the number of particles entering through the defined unit area at the laminar flow unit inlet in the simulation, the number of particles passing per unit area in the simulation results was converted into the number of particles per unit volume. Since no experimental data was available at the outlet of the laminar flow unit, the experimental measurement result from Region 6 was used instead. The reason for selecting Region 6 is that, according to the simulation results, particles pass through this region only once, making it the closest region to the values at the laminar flow unit inlet.

d) Comparison of Simulation Results with Experimental Measurements

The results of repeated simulations for 0.5 µm, 1 µm, and 5 µm particulate matter have been compared with experimental measurements through graphical representations.

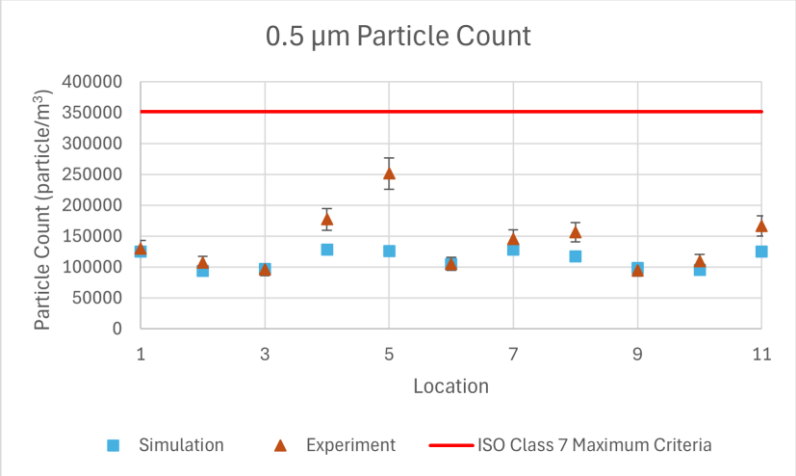

Figure 11. Comparison of simulation and experimental results with 10% error bars for 0.5 µm particles.

 doi:10.20944/preprints202507.2346.v1

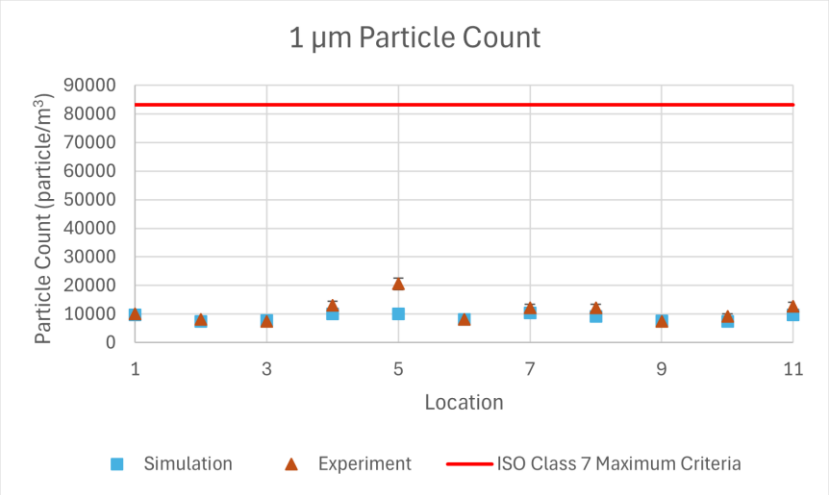

Figure 12. Comparison of simulation and experimental results with 10% error bars for 1 µm particles

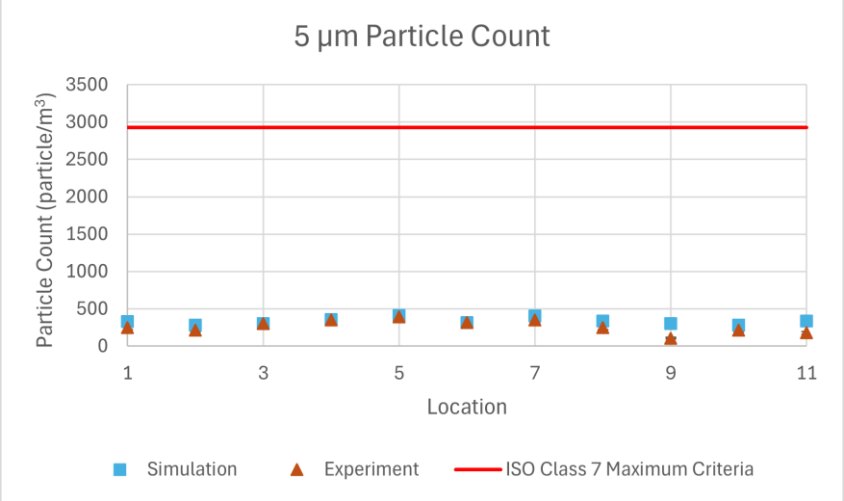

Figure 13. Comparison of simulation and experimental results with 10% error bars for 5 µm particles.

The volumetric particle count graphs obtained from the simulation results show a close similarity to the experimental results. Average error for 0.5 µm, 1 µm, and 5 µm particles are 17.3%, 17.7% and 39.7% respectively. These error percentages can be acceptable when considering 10% measurement sensitivity of device, uncertainty on calibration of device, assumptions made on simulation such as isothermal flow, spherical particle shape, no particle-particles interactions and defining single particle size for each group instead of defining a size distribution.

In the simulation results, particle counts between points 1–6 and 6–11 exhibit a symmetric distribution, which is expected since the model did not include equipment or other elements that could disrupt airflow patterns. In contrast, the experimental results reveal asymmetry at specific locations—particularly at points 5 and 7, as shown in Figures 11 and 12—likely due to the non-symmetrical placement of equipment within the actual room. To quantify this, particle concentrations at symmetric points were compared, revealing that the average variation in simulation data was minimal—2.9%, 2.8%, and 2.1% for 0.5 µm, 1 µm, and 5 µm particles, respectively. However, the experimental data showed substantially higher asymmetry, with variations of 17.2%, 18.0%, and 26.5% for the same particle sizes. This contrast underscores how real-world factors such as equipment layout can introduce localized airflow disruptions and create contamination risk zones. These findings offer practical insights for infection control by identifying areas within the operating room where interventions—such as repositioning equipment or enhancing airflow—may be necessary to reduce particle accumulation and improve overall cleanliness.

 doi:10.20944/preprints202507.2346.v1

Both the experimental and simulation results demonstrate that the particle counts meet the ISO Class 7 standards, confirming the reliability and accuracy of the airflow and particle distribution predictions within the operating room environment.

4. Conclusions

This study confirms that the simulated operating room meets the air cleanliness and pressure standards required for ISO Class 7. The alignment between experimental measurement data and simulation results demonstrates the applicability of the Computational Fluid Dynamics (CFD) model in analyzing airflow and particulate matter.

In this study, a simulation was performed with a one-time regular placement of particles at the entrance of the laminar flow unit, demonstrating that particle distribution within the room can be accurately obtained. This approach avoided excessively long solution times, which are typically caused by high particle counts in simulations with continuous particle feeding.

Such simulation studies can provide valuable insights for improving the design of the laminar flow unit and other equipment affecting airflow within the operating room. Future simulations may incorporate more detailed geometries of surgical personnel, surgical equipment, and other medical gas installations that influence the gas dynamics during an operation. Additionally, the effect of surgical personnel and equipment on airflow and particulate matter behavior could be considered in future research. Exploration of alternative turbulence models, such as the k-ω SST or LES, may also be conducted to evaluate their effectiveness in capturing more complex flow structures and improving the accuracy of airflow and contamination predictions.

Alternative inlet and outlet vent configurations in operating rooms may minimize particle accumulation in circulation areas and improve overall airflow distribution. This study serves as a useful reference for future research aimed at improving these aspects of operating room design. However, the methodology has certain limitations. A one-way coupling approach was used, where particles are influenced by airflow but do not affect it—an assumption valid only for dilute particle concentrations. Additionally, particle-particle interactions were neglected, based on the assumption of a low particle volume fraction without significant collisions or agglomeration. These simplifications may limit the applicability of the results to scenarios with higher particle loads or more complex interactions.

Furthermore, this study highlights the importance of air quality within specialized rooms, such as operating rooms, in hospital climate control systems, and provides valuable data for the literature.

In time-dependent simulation solutions, particularly in transient conditions, the number of particles can be excessively high, and the simulation duration could extend to several days. Therefore, the ability to relate Lagrangian solution results to experimental data in steady-state conditions makes this approach unique. This study is expected to serve as a pioneering reference for master's and doctoral students in the field of mechanical engineering, particularly in sustainable airflow studies.

Acknowledgements The authors thank to Siemens and IOG Engineering for providing STAR-CCM+ CFD software and Akdeniz University for providing computer resources and Private Termessos Hospital for providing experimental measurement data.

References

Aganovic A, Cao G, Stenstad LI, Skogås JG (2019) An experimental study on the effects of positioning medical equipment on contaminant exposure of a patient in an operating room with unidirectional downflow. Build Environ 165:106096. https://doi.org/10.1016/j.buildenv.2019.04.032

Annaqeeb MK, Zhang Y, Dziedzic JW, Xue K, Pedersen C, Stenstad LI, Novakovic V, Cao G (2021) Influence of surgical team activity on airborne bacterial distribution in the operating room with a mixing ventilation system: a case study at St. Olavs Hospital. J Hosp Infect 116:91–98. https://doi.org/10.1016/j.jhin.2021.08.009

 doi:10.20944/preprints202507.2346.v1

Balocco C, Petrone G, Cammarata G, Vitali P, Albertini R, Pasquarella C (2014) Indoor air quality in a real operating theatre under effective use conditions. J Biomed Sci Eng 7:866–883. https://doi.org/10.4236/jbise.2014.711086

Brohus H, Balling KD, Jeppesen D (2006) Influence of movements on contaminant transport in an operating room. Indoor Air 16:356–372. https://doi.org/10.1111/j.1600-0668.2006.00454.x

Chow TT, Wang J (2012) Dynamic simulation on impact of surgeon bending movement on bacteria-carrying particles distribution in operating theatre. Build Environ 57:68–80. https://doi.org/10.1016/j.buildenv.2012.04.010

Çoşgun A, Koyun T (2025) Assessment of indoor air quality at a university hospital using CFD and GIS. Int J Environ Sci Technol. https://doi.org/10.1007/s13762-024-06329-6

Friberg B, Friberg S, Östensson R, Burman LG (2001) Surgical area contamination—comparable bacterial counts using disposable head and mask and helmet aspirator system, but dramatic increase upon omission of head-gear: an experimental study in horizontal laminar air-flow. J Hosp Infect 47:110–115. https://doi.org/10.1053/jhin.2000.0909

Gosman AD, Ioannides E (1983) Aspects of computer simulation of liquid-fueled combustors. AIAA J Energy 7(6):482–490

Hand JL, Kreidenweis SM (2002) A new method for retrieving particle refractive index and effective density from aerosol size distribution data. Aerosol Sci Technol 36(10):1012–1026. https://doi.org/10.1080/02786820290092276

Hospodsky D, Qian J, Nazaroff WW, Yamamoto N, Bibby K, Yazdi HR, Peccia J (2012) Human occupancy as a source of indoor airborne bacteria. PLoS ONE 7(4):e34867. https://doi.org/10.1371/journal.pone.0034867

Hu M, Peng J, Sun K, Yue D, Guo S, Wiedensohler A, Wu Z (2012) Estimation of size-resolved ambient particle density based on the measurement of aerosol number, mass, and chemical size distributions in the winter in Beijing. Environ Sci Technol 46(18):9941–9947. https://doi.org/10.1021/es204073t

Kassianov E, Barnard J, Pekour M, Berg LK, Shilling J, Flynn C, et al. (2014) Simultaneous retrieval of effective refractive index and density from size distribution and light-scattering data: weakly absorbing aerosol. Atmos Meas Tech 7(10):3247–3261. https://doi.org/10.5194/amt-7-3247-2014

Khlystov A, Stanier C, Pandis SN (2004) An algorithm for combining electrical mobility and aerodynamic size distributions data when measuring ambient aerosol. Special issue of Aerosol Science and Technology on findings from the fine particulate matter supersites program. Aerosol Sci Technol 38(sup1):229–238. https://doi.org/10.1080/02786820390229543

Li CS, Hou PA (2003) Bioaerosol characteristics in hospital clean rooms. Sci Total Environ 305:169–176. https://doi.org/10.1016/S0048-9697(02)00500-4

Li Z, Wei Y, Zhang Y, Xie Y, Li L, Li K, et al. (2018) Retrieval of atmospheric fine particulate density based on merging particle size distribution measurements: multi-instrument observation and quality control at Shouxian. J Geophys Res Atmos 123:12474–12488. https://doi.org/10.1029/2018JD028956

Mackintosh CA, Lidwell OM, Towers AG, Marples RR (1978) The dimensions of skin fragments dispersed into the air during activity. J Hyg 81:471–480. https://doi.org/10.1017/S0022172400025341

Nazaroff WW (2004) Indoor particle dynamics. Indoor Air 14(7):175–183. https://doi.org/10.1111/j.1600-0668.2004.00286.x

Pasquarella C, et al. (2007) A mobile laminar airflow unit to reduce air bacterial contamination at surgical area in a conventionally ventilated operating theatre. J Hosp Infect 66:313–319. https://doi.org/10.1016/j.jhin.2007.05.022

Pasquarella C, Balocco C, Colucci ME, Saccani E, Paroni S, Albertini L, et al. (2020) The influence of surgical staff behavior on air quality in a conventionally ventilated operating theatre during a simulated arthroplasty: a case study at the University Hospital of Parma. Int J Environ Res Public Health 17:452. https://doi.org/10.3390/ijerph17020452

 doi:10.20944/preprints202507.2346.v1

Pitz M, Schmid O, Heinrich J, Birmili W, Maguhn J, Zimmermann R, et al. (2008) Seasonal and diurnal variation of PM2.5 apparent particle density in urban air in Augsburg, Germany. Environ Sci Technol 42(14):5087–5093. https://doi.org/10.1021/es7028735

Saidi MH, Sajadi B, Molaeimanesh GR (2011) The effect of source motion on contaminant distribution in the cleanrooms. Energy Build 43:966–970. https://doi.org/10.1016/j.enbuild.2010.12.021

Schiller L, Naumann A (1933) Ueber die grundlegenden Berechnungen bei der Schwerkraftaufbereitung. VDI Z 77(12):318–320

Sommerfeld M (2000) Theoretical and experimental modelling of particulate flows. Tech Rep Lecture Ser 2000-06, von Karman Institute for Fluid Dynamics, Rhode-Saint-Genèse, Belgium, pp 20–23